(Preprint) AAS 18-272

EFFECT OF CROSS-CORRELATION OF ORBITAL ERROR ON PROBABILITY OF COLLISION DETERMINATION

Steve Casali[1], Doyle Hall[1], Dan Snow[1], Matt Hejduk[2], Lauren Johnson[1], Brent Skrehart[1] and Luis Baars[1]

This paper discusses the effect of global model error on probability of collision (Pc) determination. Modifications to the Pc formulation for cross-correlation of orbital error in prediction are developed and assessed for recent conjunctions. While specific geometries can be identified or constructed to produce significant change in Pc for the modified formulation, it is of operational interest to quantify the relative occurrence of such cases for satellite conjunction risk assessment. Large-scale analysis is feasible per data collections in place over the past year.

INTRODUCTION

Probability of collision (Pc) determination between satellites requires full statistical knowledge of the underlying orbital errors. Orbital error can be broadly categorized as satellite-specific error, originating from random observational inaccuracies, for example; and globally-induced error, arising from imprecision in standard physical models. Each error source distinctly influences Pc, as has been recognized since the inception of standard alogorithms[1] for computing Pc. While prior papers have addressed this topic[2], suitable modeling and breakout of globally-induced error for Pc computation is nontrivial and sometimes presumed to be second-order in nature.

General Background

Recently, global atmospheric density forecast error was statistically characterized for an operational density model during development of a new uncertainty model for the drag consider parameter within the Astrodynamics Support Workstation (ASW). The development resulted in the Dynamic Consider Parameter (DCP) application in ASW, operationally deployed in mid-2015. Although the effort was conducted to improve satellite state covariance realism, implications for Pc determination were evident during the analysis per the connection to globally-induced error.

The drag consider parameter in ASW represents a *relative* change in predicted atmospheric density (ρ) and/or ballistic coefficient (B). It is defined strictly in prediction as a step function from the end of the orbit determination (OD) reflecting the discontinuous nature of the solar indices forecast relative to measured values. Originally, the drag consider parameter uncertainty was set to 12%, applicable to lower altitudes as for the International Space Station (ISS). DCP extended it to higher altitudes and added temporal variation with solar activity.

The methodology for DCP logically divides predicted ρ and B error into two independent components. The first represents the usually predominant error due to solar forecast inaccuracy, to include related forecast errors in the Dynamic Calibration Atmosphere (DCA) coefficients[3]. The

[1] Research Analyst, Omitron Inc., 555 E. Pikes Peak Ave, #205 Colorado Springs, CO 80903.
[2] Chief Engineer, NASA Robotic CARA, Astrorum Consulting LLC, 10006 Willow Bend Dr, Woodway, TX 76712.

second represents error due to frontal area change in prediction relative to the OD solution as manifested by B. Fourth-order polynomials for four categories of solar activity give density forecast uncertainty versus perigee height. Variable frontal area uncertainty is obtained through reductions on the ASW B histories looking back many months to one year. Each DCP component is expressed as a relative uncertainty, and the total DCP variance is the sum of the component variances assuming statistical independence. DCP is run for each drag satellite three times per day in synch with the cadence for ASW solar indices download and DCA solution. Both DCP component uncertainties are saved in growing histories by satellite.

Note that the first DCP component is globally-driven, while the second is satellite-specific. The former implies cross-correlation of orbital error between satellites, particularly given its typical predominance. This was in fact evident during the DCP evaluation, for which high correlations were observed for in-track error amongst satellites and with solar activity throughout the DCP study period. However, currently there is no means of accounting for cross-correlation of orbital error in the Pc computation from separately generated ephemerides.

Inclusion of cross-correlation effects is facilitated by the recently developed ASW-based Brute Force Monte-Carlo (BFMC) tool[4], which performs predictions of primary and secondary satellites within an execution. This allows statistically treating globally-induced drag error as distinct from satellite-specific drag error per the two DCP uncertainties, through either direct application of global error in the Monte Carlo trials themselves or as an analytical adjustment to the standard Pc, as developed below.

Study Objective

The goal herein is to develop the Pc formulation for the presence of density forecast error and related cross-correlation of orbital error. The practical effect of the resulting alterations to the standard Pc is then shown. The analysis is performed in the context of the ASW drag consider parameter and DCP per their relation to density forecast error, often the largest source of orbital inaccuracy for low-Earth satellites. Cross-correlation of orbital error stemming from mismodeling in the OD is more complicated and not treated herein, although in most cases it is expected to be the minor contributor to overall error cross-correlation.

DEVELOPMENT

The standard Pc computation is driven by the miss vector at time of closest approach (TCA) and its associated covariance, as determined from estimates of primary and secondary state and covariance. The miss vector is just the positional difference to the secondary from the primary at TCA, and the miss vector covariance is a combination of primary and secondary covariance. The miss vector covariance is often referred to as the joint covariance and is developed below using the following definitions, with bold indicating vectors or matrices and dimensions (dim) indicated.

- $\mathbf{r}$ = variable denoting position vector at TCA (dim 3)
- $\boldsymbol{\mu}$ = variable denoting a posteriori mean (estimate) of $\mathbf{r}$ (dim 3)
- $\mathbf{P}$ = variable denoting a posteriori covariance matrix of $\mathbf{r}$ (dim 3 by 3)
- δ = variable denoting epoch state error (dim state size n)
- $\boldsymbol{\Phi}$ = variable denoting positional state transition matrix (dim 3 by n), mapping deviation in epoch state to position deviation at TCA
- $\mathbf{G}$ = variable denoting positional global model parameter transition vector (dim 3), mapping deviation in Δ (below) to position deviation at TCA
- Δ = variable denoting global model parameter error
- σ = variable denoting a priori (empirical) sigma of Δ

p = subscript denoting primary satellite
s = subscript denoting secondary satellite
m = subscript denoting miss vector at TCA
g = subscript denoting global model parameter
e = subscript denoting epoch variable

From the definition of miss vector ($\mathbf{r}_m = \mathbf{r}_s - \mathbf{r}_p$), its mean ($\boldsymbol{\mu}_m$), and covariance ($\mathbf{P}_m$), with E denoting the expected value operator,

$$\boldsymbol{\mu}_m = E[\mathbf{r}_m] = E[\mathbf{r}_s - \mathbf{r}_p] = E[\mathbf{r}_s] - E[\mathbf{r}_p] = \boldsymbol{\mu}_s - \boldsymbol{\mu}_p \tag{1}$$

$$\mathbf{P}_m = E\left[(\mathbf{r}_m - \boldsymbol{\mu}_m)(\mathbf{r}_m - \boldsymbol{\mu}_m)^T\right] = E\left[((\mathbf{r}_s - \boldsymbol{\mu}_s) - (\mathbf{r}_p - \boldsymbol{\mu}_p))((\mathbf{r}_s - \boldsymbol{\mu}_s) - (\mathbf{r}_p - \boldsymbol{\mu}_p))^T\right] \tag{2}$$

$$\begin{aligned}\mathbf{P}_m = {} & E\left[(\mathbf{r}_s - \boldsymbol{\mu}_s)(\mathbf{r}_s - \boldsymbol{\mu}_s)^T\right] + E\left[(\mathbf{r}_p - \boldsymbol{\mu}_p)(\mathbf{r}_p - \boldsymbol{\mu}_p)^T\right] \\ & - E\left[(\mathbf{r}_s - \boldsymbol{\mu}_s)(\mathbf{r}_p - \boldsymbol{\mu}_p)^T\right] - E\left[(\mathbf{r}_p - \boldsymbol{\mu}_p)(\mathbf{r}_s - \boldsymbol{\mu}_s)^T\right]\end{aligned} \tag{3}$$

$$\mathbf{P}_m = \mathbf{P}_s + \mathbf{P}_p - E\left[(\mathbf{r}_s - \boldsymbol{\mu}_s)(\mathbf{r}_p - \boldsymbol{\mu}_p)^T\right] - E\left[(\mathbf{r}_p - \boldsymbol{\mu}_p)(\mathbf{r}_s - \boldsymbol{\mu}_s)^T\right] \tag{4}$$

where the last relation results from the definition of primary and secondary covariance ($\mathbf{P}_p$, $\mathbf{P}_s$), analogous to the first relation in Eq. (1) for $\boldsymbol{\mu}_m$ in terms of primary and secondary mean ($\boldsymbol{\mu}_p$, $\boldsymbol{\mu}_s$).

Normally, the two subtractive terms in $\mathbf{P}_m$ are assumed to be zero in the standard Pc computation, with the joint covariance simply given as the sum of primary and secondary covariance. This is justified if the orbital errors from orbit determination and prediction of the two satellites are statistically independent. Relating a position deviation at TCA to a deviation in epoch state via the state transition matrix

$$\mathbf{r}_s - \boldsymbol{\mu}_s = \boldsymbol{\Phi}_s \boldsymbol{\delta}_s \quad \text{and} \quad \mathbf{r}_p - \boldsymbol{\mu}_p = \boldsymbol{\Phi}_p \boldsymbol{\delta}_p \tag{5}$$

readily implies the subtractive terms in the expression for $\mathbf{P}_m$ are in fact zero if errors in the orbit determination are independent with $E[\boldsymbol{\delta}_s \boldsymbol{\delta}^T_p] = 0$, and no common prediction errors are present.

The point of the current analysis is to consider the case where common prediction errors *are* present. This implies generalizing the above error relations to include a global model parameter error Δ_g acting purely in prediction, representable in its simplest form as

$$\mathbf{r}_s - \boldsymbol{\mu}_s = \boldsymbol{\Phi}_s \boldsymbol{\delta}_s + \mathbf{G}_s \Delta_g \quad \text{and} \quad \mathbf{r}_p - \boldsymbol{\mu}_p = \boldsymbol{\Phi}_p \boldsymbol{\delta}_p + \mathbf{G}_p \Delta_g \tag{6}$$

where state transition vector $\mathbf{G}$ (satellite dependent) gives the linearized effect of scalar Δ_g on predicted position over the course of state propagation from epoch, analogous to $\boldsymbol{\Phi}$. Substitution into the general expression for $\mathbf{P}_m$ in Eq. (3) gives

$$\begin{aligned}\mathbf{P}_m = {} & E\left[(\boldsymbol{\Phi}_s \boldsymbol{\delta}_s + \mathbf{G}_s \Delta_g)(\boldsymbol{\Phi}_s \boldsymbol{\delta}_s + \mathbf{G}_s \Delta_g)^T\right] + E\left[(\boldsymbol{\Phi}_p \boldsymbol{\delta}_p + \mathbf{G}_p \Delta_g)(\boldsymbol{\Phi}_p \boldsymbol{\delta}_p + \mathbf{G}_p \Delta_g)^T\right] \\ & - E\left[(\boldsymbol{\Phi}_s \boldsymbol{\delta}_s + \mathbf{G}_s \Delta_g)(\boldsymbol{\Phi}_p \boldsymbol{\delta}_p + \mathbf{G}_p \Delta_g)^T\right] - E\left[(\boldsymbol{\Phi}_p \boldsymbol{\delta}_p + \mathbf{G}_p \Delta_g)(\boldsymbol{\Phi}_s \boldsymbol{\delta}_s + \mathbf{G}_s \Delta_g)^T\right]\end{aligned} \tag{7}$$

Again assuming the OD states are independent ($E[\boldsymbol{\delta}_s \boldsymbol{\delta}^T_p] = 0$) and naturally assuming global error acting in prediction is independent of epoch errors ($E[\boldsymbol{\delta}_s \Delta_g] = 0 = E[\boldsymbol{\delta}_p \Delta_g]$), leads to a more complete form for $\mathbf{P}_m$ with $\sigma^2_g = E[\Delta^2_g]$

$$\mathbf{P}_m = \boldsymbol{\Phi}_s \mathbf{P}_{s/e} \boldsymbol{\Phi}^T_s + \boldsymbol{\Phi}_p \mathbf{P}_{p/e} \boldsymbol{\Phi}^T_p + \sigma^2_g (\mathbf{G}_s \mathbf{G}^T_s + \mathbf{G}_p \mathbf{G}^T_p - \mathbf{G}_s \mathbf{G}^T_p - \mathbf{G}_p \mathbf{G}^T_s) \tag{8}$$

$$\mathbf{P}_m = \mathbf{P}_s + \mathbf{P}_p - \sigma^2_g (\mathbf{G}_s \mathbf{G}^T_p + \mathbf{G}_p \mathbf{G}^T_s) \tag{9}$$

where $\mathbf{P}_{p/e}$ and $\mathbf{P}_{s/e}$ are the primary and secondary covariances at epoch representing errors in $\boldsymbol{\delta}$.

For this application, Δ_g represents a relative change in density ρ during prediction with respect to model density per the ASW definition of drag consider parameter. As such, Δ_g and σ_g reflect just the density forecast component of DCP. Further, Δ_g is equivalent to a relative change in B through the ρB term in drag acceleration, and because ASW solves for B as a relative correction, $\mathbf{G}$ is the B column of $\mathbf{\Phi}$. This mathematically allows for simply increasing the B variance of $\mathbf{P}_{s/e}$ and $\mathbf{P}_{p/e}$ by σ^2_g to give the additive σ^2_g terms (versus separately mapping and adding). Moreover, DCP frontal area variance is also naturally added the same way to $\mathbf{P}_{s/e}$ and $\mathbf{P}_{p/e}$ being satellite-specific and B-induced. Since the two DCP component variances sum to the full DCP variance, the result is the total DCP variance is added to epoch B variance for each satellite to yield the additive terms of $\mathbf{P}_m$ comprised by $\mathbf{P}_s$ and $\mathbf{P}_p$ in Eq. (9).

Therefore, the DCP density forecast component is currently reflected in $\mathbf{P}_m$ through just the additive terms of Eq. (9) but not the subtractive terms. In other words, global uncertainty is included but applied independently to the two satellites through epoch B variance in separate satellite predictions. The result is $\mathbf{P}_m$ may be inflated, depending on the relative contributions of the terms. Usually some inflation in $\mathbf{P}_m$ is conservative and acceptable, but in other cases, it can decrease Pc.

Finally, the general expression for $\mathbf{P}_m$ is actually a little more complicated than stated because the global density error affects the two satellites slightly differently. Because DCP varies with perigee height, the satellites generally will have different DCP density forecast uncertainties if they differ in perigee height. However, this is usually a lesser effect, particularly for near-circular orbits, and the adjustments needed to $\mathbf{P}_m$ to account for it are minor. Rather than a single σ^2_g term, $\sigma^2_{s/g}$, $\sigma^2_{p/g}$, and $(\sigma_{s/g}\ \sigma_{p/g})$ terms appear in the global contributions, with similar values typically, where the extra s and p subscripts denote some dependency of global density error uncertainty on the secondary and primary orbits. This can be seen through creating a generalized dependency in Eq. (7) for Δ_g as $\Delta_{s/g} = \sigma_{s/g}\ x$ and $\Delta_{p/g} = \sigma_{p/g}\ x$, where x is an unbiased random variable with unity variance and again uncorrelated to epoch state error (δ). Making this generalization gives

$$\mathbf{P}_m = \mathbf{\Phi}_s\,\mathbf{P}_{s/e}\,\mathbf{\Phi}^T_s + \mathbf{\Phi}_p\,\mathbf{P}_{p/e}\,\mathbf{\Phi}^T_p + \sigma^2_{s/g}\,\mathbf{G}_s\,\mathbf{G}^T_s + \sigma^2_{p/g}\,\mathbf{G}_p\,\mathbf{G}^T_p - \sigma_{s/g}\,\sigma_{p/g}\,\mathbf{G}_s\,\mathbf{G}^T_p - \sigma_{s/g}\,\sigma_{p/g}\,\mathbf{G}_p\,\mathbf{G}^T_s \quad (10)$$

$$\mathbf{P}_m = \mathbf{P}_s + \mathbf{P}_p - \sigma_{s/g}\,\sigma_{p/g}\,\mathbf{G}_s\,\mathbf{G}^T_p - \sigma_{s/g}\,\sigma_{p/g}\,\mathbf{G}_p\,\mathbf{G}^T_s \quad (11)$$

General Implications

Several inferences can be drawn on the effect the global density error Δ_g and its statistics have on the miss vector covariance $\mathbf{P}_m$. For notational clarity, the simpler form for $\mathbf{P}_m$ in Eq. (9) is initially discussed, though the results extend analogously to the more general form for $\mathbf{P}_m$ in Eq. (11) as given subsequently. Several additional quantities are required below and further expounded during the discussion to follow:

- $\mathbf{v}$ = variable denoting a velocity vector at TCA
- k = variable denoting a drag sensitivity scalar
- r = subscript denoting relative velocity at TCA
- o = subscript denoting orthogonal velocity at TCA

First, the basic form for $\mathbf{P}_m$ can be restated as

$$\mathbf{P}_m = \mathbf{\Phi}_s\,\mathbf{P}_{s/e}\,\mathbf{\Phi}^T_s + \mathbf{\Phi}_p\,\mathbf{P}_{p/e}\,\mathbf{\Phi}^T_p + \sigma^2_g\,(\mathbf{G}_s - \mathbf{G}_p)\,(\mathbf{G}_s - \mathbf{G}_p)^T \quad (12)$$

which also readily follows from performing the preceding reduction starting from the miss vector:

$$\mathbf{r}_m - \boldsymbol{\mu}_m = (\mathbf{r}_s - \boldsymbol{\mu}_s) - (\mathbf{r}_p - \boldsymbol{\mu}_p) \tag{13}$$

$$\mathbf{r}_m - \boldsymbol{\mu}_m = \boldsymbol{\Phi}_s \boldsymbol{\delta}_s + \mathbf{G}_s \Delta_g - \boldsymbol{\Phi}_p \boldsymbol{\delta}_p - \mathbf{G}_p \Delta_g \tag{14}$$

$$\mathbf{r}_m - \boldsymbol{\mu}_m = \boldsymbol{\Phi}_s \boldsymbol{\delta}_s - \boldsymbol{\Phi}_p \boldsymbol{\delta}_p + \Delta_g (\mathbf{G}_s - \mathbf{G}_p) \tag{15}$$

These arrangements illustrate the one-dimensional effect of Δ_g and its associated statistics in $\mathbf{P}_m$, where it is seen to contribute a covariance of rank one given by $\sigma^2_g (\mathbf{G}_s - \mathbf{G}_p) (\mathbf{G}_s - \mathbf{G}_p)^T$.

Further insight can be gleaned in considering the specific effect drag has on TCA position in the context of Pc computation. As commonly accepted, the dominant effect of drag is in the velocity direction, neglecting smaller variations in height and out-of-plane, to where to first-order $\mathbf{G} = k\,\mathbf{v}$. In other words, deviations in Δ_g translate into a positional change along $\mathbf{v}$ at TCA according to a satellite-dependent proportionality variable k (implicitly containing $v = |\mathbf{v}|$):

$$\mathbf{G}_s = k_s \mathbf{v}_s \quad \text{and} \quad \mathbf{G}_p = k_p \mathbf{v}_p \tag{16}$$

This means (Eq. (15)) deviations in miss vector due to Δ_g are simply given by $\Delta_g (k_s \mathbf{v}_s - k_p \mathbf{v}_p)$. Moreover, during rotation to the collision plane perpendicular to relative velocity in the Pc formulation, errors along relative velocity are rotated out. This leads to only the components of $\mathbf{v}_s$ and $\mathbf{v}_p$ orthogonal to the relative velocity ($\mathbf{v}_r = \mathbf{v}_s - \mathbf{v}_p$) as relevant to the projection of $\mathbf{P}_m$ in the collision plane and hence to Pc. Furthermore, $\mathbf{v}_s$ and $\mathbf{v}_p$ share the same orthogonal component $\mathbf{v}_o$ in the plane of the velocities, as evident geometrically from the diagram

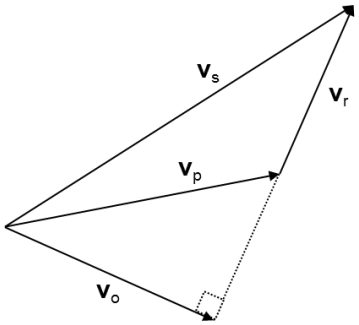

Figure 1. Relative Velocity Illustration

Therefore, the effect of Δ_g on $\mathbf{r}_m$ in the collision plane is just $\Delta_g (k_s - k_p) \mathbf{v}_o$, to where its statistical effect on the projection of $\mathbf{P}_m$ in the collision plane is $\sigma^2_g (k_s - k_p)^2 \mathbf{v}_o \mathbf{v}_o^T$. Furthermore, it follows analogously that taking into account satellite dependency in the statistics of Δ_g just modifies the expression for the statistical effect to be $(\sigma_{s/g} k_s - \sigma_{p/g} k_p)^2 \mathbf{v}_o \mathbf{v}_o^T$. Similar to Eq. (11), this can be seen through adding a generalized dependency in Eq. (15) for Δ_g as $\Delta_{s/g} = \sigma_{s/g}\, x$ and $\Delta_{p/g} = \sigma_{p/g}\, x$, where x is an unbiased random variable with unity variance. The general result then follows from Eq. (15) and Eq. (16) and taking the expected value of $(\mathbf{r}_m - \boldsymbol{\mu}_m)(\mathbf{r}_m - \boldsymbol{\mu}_m)^T$.

Several key points emerge regarding the influence of global density error uncertainty on Pc through its effect on the projection of $\mathbf{P}_m$ in the collision plane. These are in line with intuition prior to the analysis but are more apparent upon reduction and dynamical simplification as above.

First, the effect on Pc is negligible when $\mathbf{v}_o$ is small or zero, in line with intuition that head-on conjunctions are relatively unaffected, with the main change then being TCA uncertainty. Second, if sensitivity to drag is low (e.g. small energy dissipation rate (EDR), which is given a more formal description in the following section, or short propagation), as reflected in the proportional-

ity variable k, the effect is comparatively small, as also intuitively evident. Similarly, if global density error variance σ^2_g is small or assumed negligible, the effect trivially vanishes.

Third and more interestingly, if the drag sensitivities are comparable or identical for the two satellites, through some combination of EDR and propagation time, the effect again vanishes, even for significant drag cases. This was understood prior as the example of a "crossing" conjunction with similar drag uncertainty dispersions that might behave in tandem for a perfectly correlated error source. For this case, the implication is that global uncertainty needs no inclusion, akin to not applying the main DCP component (density forecast uncertainty) of the drag consider parameter variance at all.

This raises the fourth point mentioned previously that applying DCP independently by satellite without breaking out global and satellite-specific error can lead to inflation of the joint covariance and its projection in the collision plane. The current process essentially applies $(k^2_s + k^2_p)$ in the above, versus $(k_s - k_p)^2 = k^2_s + k^2_p - 2\, k_s\, k_p$, in processing satellites independently, with the subtractive term omitted. This observation holds for both the simpler and more general expressions for $\mathbf{P}_m$ in σ_g and $(\sigma_{p/g}, \sigma_{s/g})$.

In summary to this point, the complete form for the joint covariance of the miss vector has been derived and discussed for the influence of a global relative density error per Eq. (9) and Eq. (11), where certain cross correlation error terms normally assumed to be zero arise in the formulation. The effect of these terms is to decrease the size of the joint covariance relative to that produced by separate application of drag consider parameter variance to primary and secondary satellites. Scenarios are readily identifiable for close conjunctions where applying the subtractive terms could raise Pc, while for other cases with larger miss vectors, the current Pc is conservative due to effective inflation.

EDR Approximation

Further approximation along the lines of the above velocity form for **G** utilizing EDR and prediction time (t) is possible. EDR is a composite measure of the level of drag acting on a satellite, encompassing all drag acceleration parameters in density, velocity, B, etc. Instantaneous EDR is simply the negative dot product of velocity ($\mathbf{v}$) and drag acceleration ($\mathbf{a}_D$) from the physical definition of rate of change of specific energy, with average EDR over an OD or prediction interval reported by ASW. Being directly connected to orbital energy, EDR is relatable to the dominant in-track drag effect on semi-major axis (a) and mean-motion (n), as outlined below in terms of t, change in mean-anomaly (ΔM) due to drag, and Earth gravitational constant μ.

With an overhead dot denoting the time rate of change of a variable, Lagrange's Planetary equations[5] show $\dot{a}$ is proportional to the dot product of $\mathbf{v}$ and $\mathbf{a}_D$ (considering drag only), which also follows from differentiation of the two-body energy equation. Given the close relation between $\dot{n}$ and $\dot{a}$ found from differentiating $n^2 a^3 = \mu$, it follows that EDR is proportional to $\dot{n}/2$ and thus to quadratic mean-anomaly change per $\Delta M = (\dot{n}/2)\, t^2$ (from general perturbations (GP) theory). Lastly, a deviation in mean-anomaly corresponds to a deviation along $\mathbf{v}$ by an elapsed $\Delta t = \Delta M/n$. This progression is summarized as

$$v^2/2 = \mu/r - \mu/2a \quad \rightarrow \quad \dot{a} = (2a^2/\mu)\, \mathbf{v} \cdot \mathbf{a}_D \quad \rightarrow \quad \dot{a} = (-2a^2/\mu)\, EDR \tag{17}$$

$$n^2 a^3 = \mu \quad \rightarrow \quad 2\, n\, \dot{n}\, a^3 + 3\, n^2\, a^2\, \dot{a} = 0 \quad \rightarrow \quad \dot{a}/a = -\, 2/3\, (\dot{n}/n) \tag{18}$$

$$\dot{n} = (3\, n\, a\, /\, \mu)\, EDR \quad \rightarrow \quad \dot{n}/2 = 3/2\, EDR\, /\, \sqrt{(\mu\, a)} \quad \rightarrow \quad \Delta M = 3/2\, EDR\, t^2\, /\, \sqrt{(\mu\, a)} \tag{19}$$

$$\Delta \mathbf{r} = (\Delta M/n)\, \mathbf{v} = \mathbf{v}\, \{\, 3/2\, EDR\, t^2\, /\, \sqrt{(\mu\, a)}\, \}\, /\, n \tag{20}$$

Therefore, Eq. (20) relates EDR and prediction time to a positional change due to drag at TCA. This sensitivity relation is what the prior model transition vector **G** represents. The only remaining step is to recognize that relative changes in density and B translate into relative changes in EDR since drag acceleration $\mathbf{a}_D$ is proportional to each. Therefore, **G** is simply given by $\Delta\mathbf{r}$ from Eq. (20), meaning a deviation in **r** due to a relative global density variation is simply $\Delta\mathbf{r}\,\Delta_g$.

ANALYSIS

To address the practical effect of the cross correlation of orbital error due to predicted density error, recent conjunctions from the Conjunction Assessment Risk Analysis (CARA) database were examined in the BFMC framework. The conjunctions comprise data from the Conjunction Data Message (CDM) and associated primary and secondary Vector Covariance Message (VCM) containing epoch state and model. In support of the VCM, CARA has been collecting corresponding environmental data to fully reproduce operational scenarios since spring 2016, although the complete datasets needed for this purpose were not finalized until spring 2017. This data includes both DCP uncertainty components as well as the model-compatible B, solar indices, and DCA coefficients, to where recent conjunctions of interest should be fully assessable.

However, off-line reproduction of an operational scenario is not always straightforward or possible, mainly because of inherent timing issues in the data capture process for the VCMs and environmental data occurring approximately once per shift and for high-interest conjunctions to where the environmental data in effect for a conjunction cannot always be automatically identified. Therefore, some conjunctions require manual reconstruction to ensure BFMC assess the correct operational scenario. Moreover, the CARA database currently does not distinguish between VCMs with the same epoch time (keeping just the latest VCM), so the satellite state needed to reproduce a conjunction may not be available. Such occurrences are not rare operationally, as analysts can produce multiple updates with the same epoch time in order to fine-tune a high-interest conjunction. Finally, reproducibility aside, the required database retrieval and conjunction verification is time consuming.

For these reasons, in addition to evaluating cross correlation within the BFMC framework of full special perturbations (SP), the effect was also assessed through CDM analysis and approximations to the drag dynamics discussed above. This allowed for quicker turnaround in gaining initial insight into the degree and scope of the effect across hundreds of conjunctions than is possible from the full SP BFMC process. To this end, EDR and prediction times directly available in the CDM were utilized to approximate the drag dynamics from epoch to TCA, as given in Eq. (20). Since DCP information is not present in the CDM, and given the approximate nature of Eq. (20), this analysis was conducted as a Pc variation across a range of sample DCP density forecast uncertainties. A full SP assessment applying actual DCP data for each conjunction followed this preliminary CDM analysis once the overall effect was evident.

Altogether, the analysis consisted of preliminary CDM testing leading into a broader full SP assessment. The latter evaluation was itself broken into two sets. The first focused on conjunctions with elevated drag, while the second considered the larger set of non-trivial drag (defined below). These runs determined Pc two ways, as current Pc without adjusting for cross-correlation and modified Pc adjusting for cross-correlation, per the joint covariance form in Eq. (11) and Eq. (9).

Finally, as a basic analysis check, a general Monte Carlo BFMC run was performed for several sample conjunctions identified within the full SP runs. For this test, BFMC was modified to perform an extra random draw explicitly for density forecast error and apply it to both satellites according to its DCP ρ variance, as described for Eq. (11) via random variable x and associated $\Delta_{p/g}$ and $\Delta_{s/g}$. The DCP B variances (only) were applied individually to epoch covariance as usual.

Analysis Data

Recent conjunctions over approximately the past year were of primary interest, which also coincides when the full SP data for BFMC started to become available just before April 1, 2017. Otherwise, the study would have also considered further back into the solar cycle closer to solar maximum, versus the near solar minimum currently in effect. Several hundred conjunctions were desired to infer the prevalence and significance of the cross-correlation effect.

The preliminary CDM testing consisted of all CDMs in the CARA database over 2017 with both primary and secondary EDR > 0.0006 W/kg (EDR Bin > 1) to consider just cases possessing clear drag dynamics, resulting in approximately 440 conjunctions. The subsequent full SP analysis for the elevated drag set, using the same EDR definition as the CDM testing, also considered about a year of conjunctions from April 2017 to April 2018, resulting in approximately 250 useable conjunctions. The full SP analysis on the non-trivial range of drag with EDR > 0.00001 W/kg for either satellite (and neither EDR zero) considered only about 4 months of recent conjunctions, resulting in about 2700 useable conjunctions. The latter set was restricted to a few months to maintain a manageable sample size, particularly during solar minimum, when a large percentage of satellites experience diminished (EDR Bin 1) levels of drag.

Also to maintain a sample of interest, only conjunctions with standard Pc > 10^{-6} were considered for the elevated drag cases, for both CDM and full SP tests. For the full SP non-trivial drag case, Pc > 10^{-5} was considered as a compromise with sample size reasonableness. (Initially queries with Pc > 10^{-6} over the past year for non-trivial drag conjunctions resulted in over 20,000 cases, an unwieldy number.) Finally, in all cases, the hard-body-radius was set to a representative 20 m, since relative Pc versus absolute Pc was of interest in the results to follow, except for the ISS, for which 70 m was invoked.

Analysis Results

The results of the preliminary CDM analysis are shown in Figure 2, which illustrates the effect of cross-correlated orbital error on standard Pc across a range of hypothetical DCP density forecast uncertainties. Being just hypothetical, the generic term of global consider parameter (GCP) for σ_g in Eq. (9) denotes the curves in Figure 2. Here, standard Pc, also known as 2D-Pc, refers to Pc found by linear reductions to the collision plane and subsequent quadrature over a 2D circular area defined by the (combined) hard-body-radius.

In Figure 2, the y-axis is the ratio of 2D-Pc accounting for cross-correlation per Eq. (9) relative to 2D-Pc that omits the subtractive terms in Eq. (9). The x-axis is conjunction instance expressed as a ratio to the total number of conjunctions for a given GCP. The total number varies by GCP because as GCP rises, it becomes increasingly unrealistic for lower altitude satellites, as reflected in the CDM B variance containing the actual DCP variance, which tends to fall with altitude. (GCP variance cannot exceed CDM relative B variance.) Therefore, sample sizes for GCP = 12% and GCP = 15% fell noticeably to 390 and 270, respectively, from the 440 for GCP = 5%, with only a small drop-off occurring for GCP = 8% and GCP = 10%. Finally, each curve is rank-ordered individually by Pc ratio value (vertical slices do not represent the same conjunction).

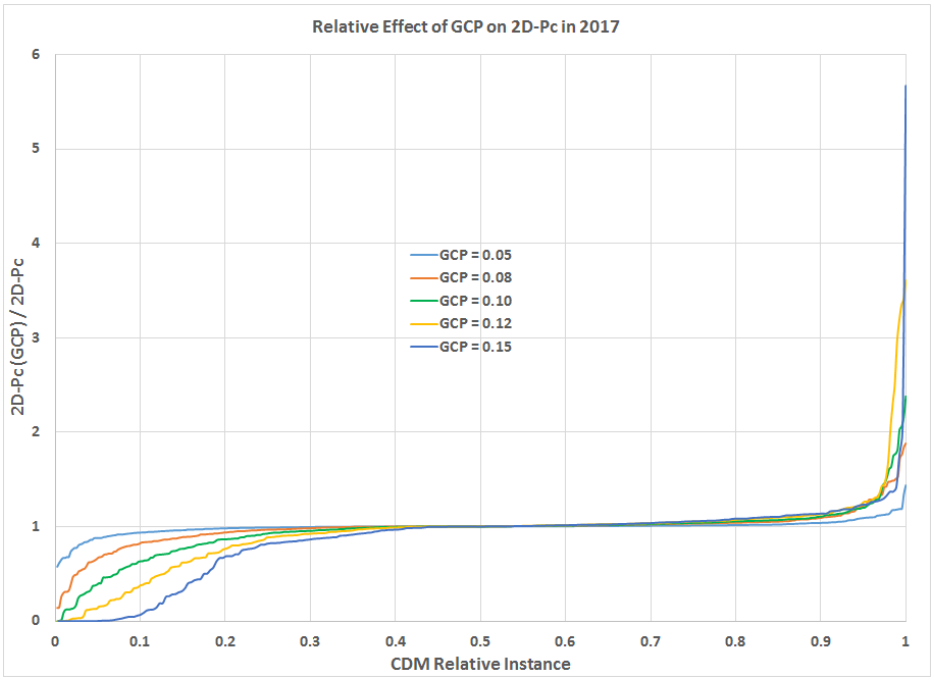

Figure 2. Preliminary CDM Analysis Results

Figure 2 implies there is substantial effect due to the cross-correlation of orbital errors in prediction, which was a logical prerequisite for performing the more extensive full SP analysis. As GCP increases, the disparity between adjusted and unadjusted 2D-Pc also increases. GCP = 5% has minor impact on Pc, while GCP = 15% is much more pronounced, especially for the smaller ratios, where a significant number of conjunctions show a drop in Pc to zero or near zero (almost 10%). However, on the other side of the plot, only relatively few conjunctions exhibit more than a factor of 2 disparity (under 5%).

Results of the full SP assessment follow in Figure 3 through Figure 8. Similar to Figure 2, these show the ratio of 2D-Pc modified for cross correlation per Eq. (11) relative to current 2D-Pc. Since these SP runs replicated the actual conjunctions with the true DCP, there is only one conjunction per point (no GCP range). Also, in addition to rank-ordered plots, the ratio is shown versus current 2D-Pc to better identify the ratios in the Pc range of prime interest above about 10^{-5}.

Figure 3 through Figure 5 show results for the elevated drag case (EDR Bin > 1) by rank-order and 2D-Pc respectively, with the last on a logarithmic scale to better discern the smallest values. The trend is similar to that of Figure 2 for GCP = 15%, but more pronounced, with fewer ratios near unity and about 20% near zero at the lower end of the ratio. As in Figure 2, relatively few ratios, under 5%, are above about 2, though significant disparities can occur at the higher end.

Figure 6 through Figure 8 show results analogous to Figure 3 through Figure 5 for the non-trivial drag case (EDR Bin $\geq$ 1). These more general drag results also encompass many elevated drag cases. The results show a much larger swath of ratios near unity, as expected, since EDR Bin 1 contains many objects with EDR approaching the trivial cutoff of 10^{-5}. Otherwise, the general trends are very similar to those of the elevated drag conjunctions, with a few even more pronounced ratios above 2 (up to 9).

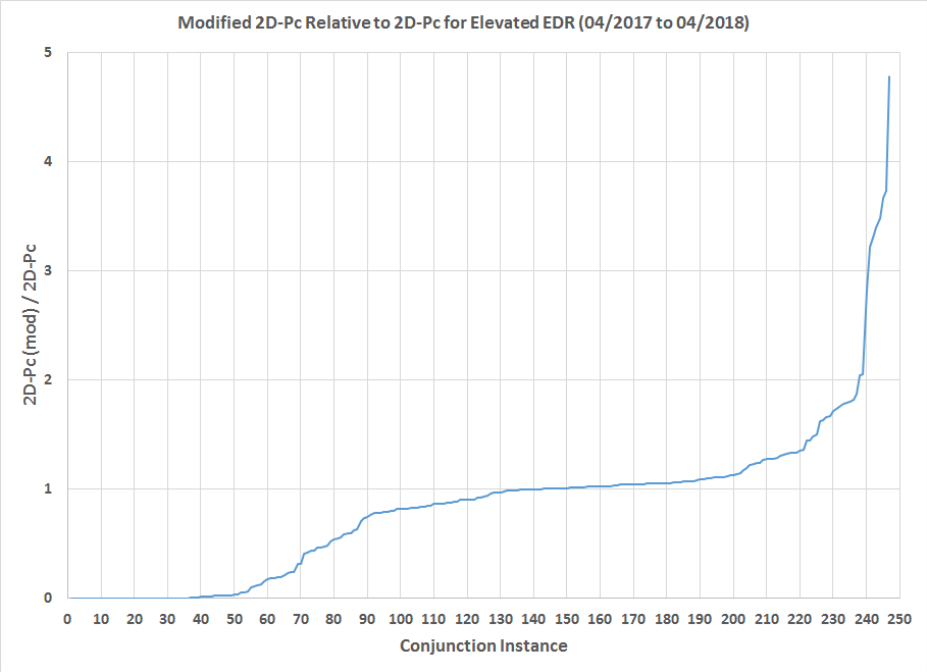

Figure 3. SP Assessment Results for Elevated Drag by Instance

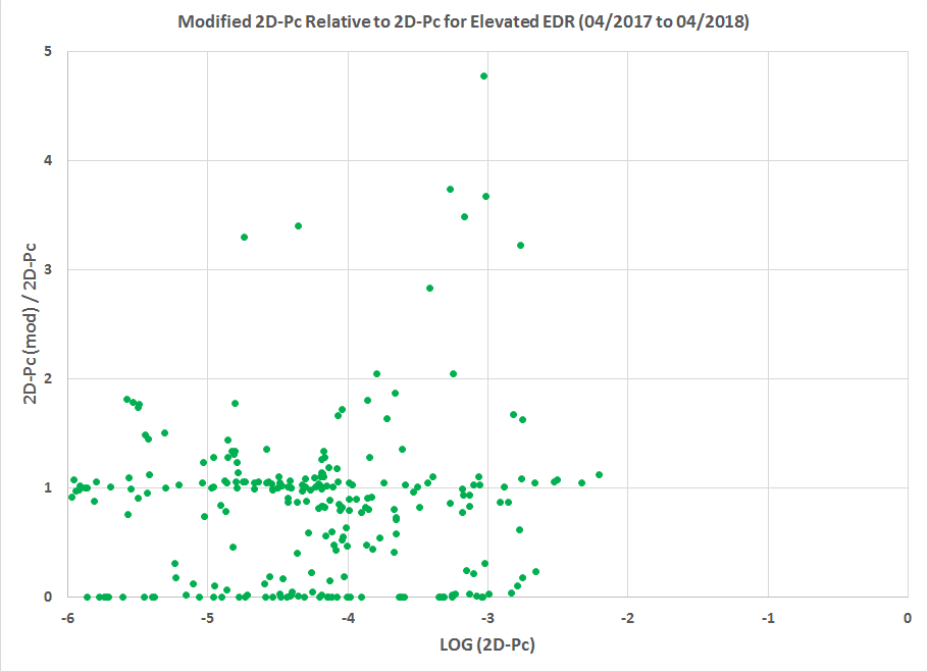

Figure 4. SP Assessment Results for Elevated Drag by 2D-Pc

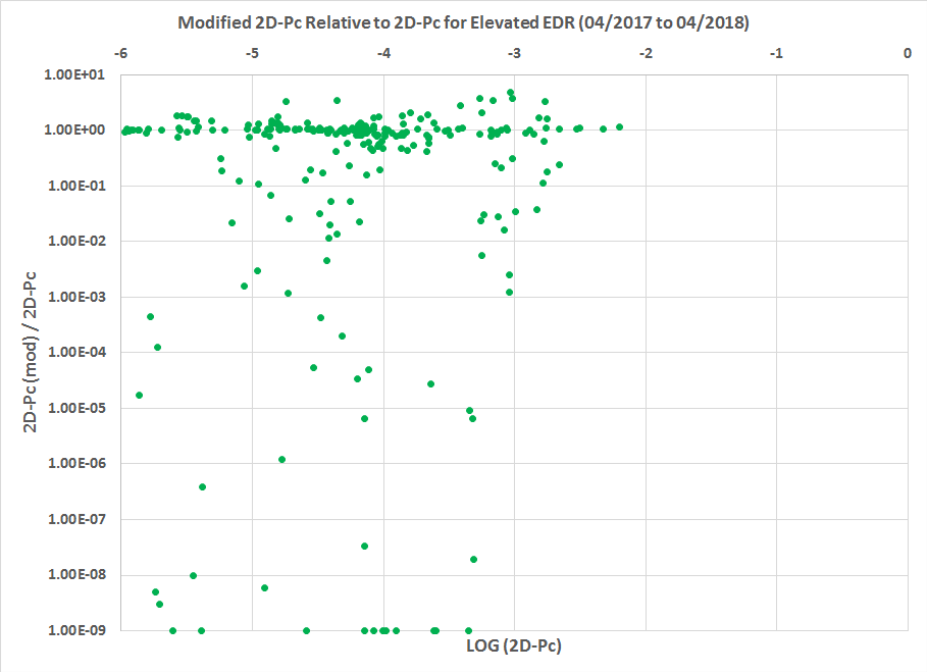

Figure 5. SP Assessment Results for Elevated Drag by 2D-Pc (Rescaled)

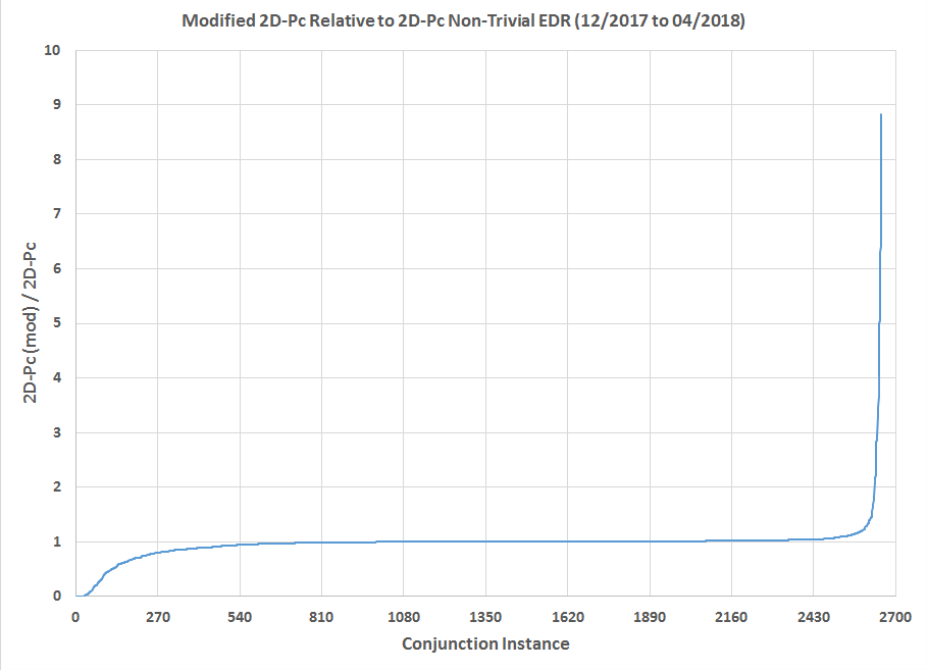

Figure 6. SP Assessment Results for Non-Trivial Drag by Instance

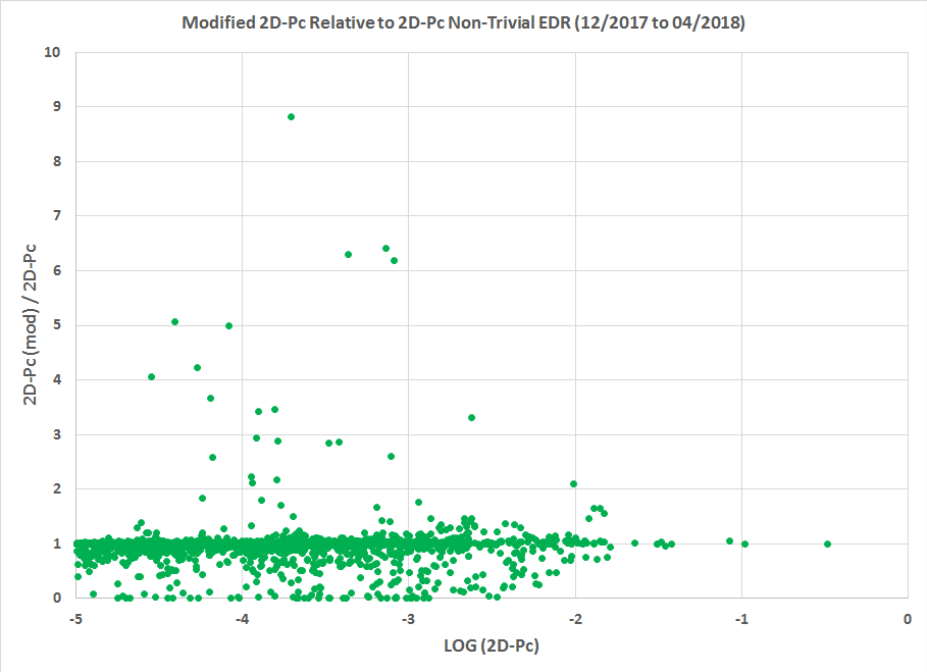

Figure 7. SP Assessment Results for Non-Trivial Drag by 2D-Pc

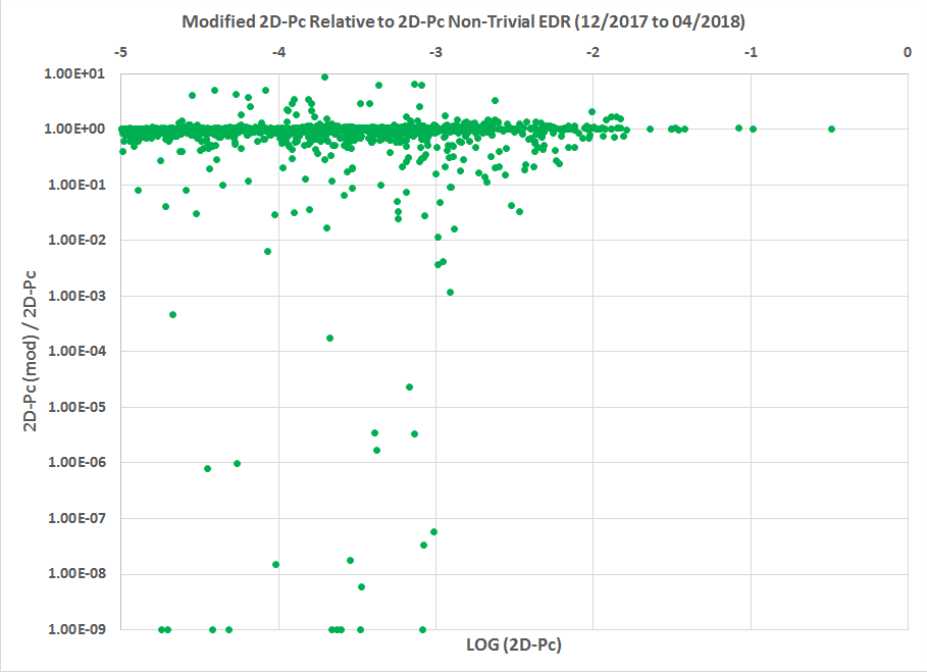

Figure 8. SP Assessment Results for Non-Trivial Drag by 2D-Pc (Rescaled)

Finally, four cases were selected for the previously mentioned full-SP Monte Carlo testing in a version of BFMC modified to make a single density forecast error draw applied to both satellites. These cases exhibited ratios (r) of modified 2D Pc to 2D Pc, shown in Figure 3 through Figure 8, ranging from very small to fairly sizeable. The cases consisted of

r = 0.0 (2D Pc = 4.8E-4) with vanishing modified 2D Pc,
r = 0.3 (2D Pc = 9.6E-4) with significantly under unity ratio,
r = 1.7 (2D Pc = 1.5E-3) with somewhat larger than unity ratio,
r = 8.8 (2D Pc = 2.0E-4) with substantially larger than unity ratio.

Since the modified 2D Pc was not statistically measurable for the first case, this test simply consisted of performing one million Monte Carlo trials to verify no hard-body-radius violation occurred, as was indeed the case. For the remaining three cases, the number of Monte Carlo trials was chosen commensurate with modified 2D-Pc to obtain a 95% confidence interval of less than 10% of modified 2D-Pc. For all three cases, the Monte Carlo results came back well within this general tolerance, which though somewhat loose compared to the rigorous BFMC testing currently underway in parallel, lent further confirmation and a sanity check to the overall formulation and analysis herein.

CONCLUSIONS

The purpose of this study has been to develop and assess the effect of cross correlation of orbital error on Pc through the action of a global density forecast error source in prediction, consistent with the current ASW drag consider parameter and associated DCP uncertainty model. To this end, a generalized joint covariance for Pc determination accounting for cross-correlated orbital error has been developed and applied to numerous recent actual conjunctions. Accompanying inferences have been made on the implications for Pc based on orbital and drag characteristics, and an EDR-based approximation to the problem has been presented. Overall, the study has successfully assessed the question from concept to application, with BFMC being instrumental in the analysis through its process for semi-automatic conjunction reproduction and assessment.

Overall, the results are in line with the anticipation that accounting for cross-correlation of orbital error tends to lower Pc due to its general deflation effect on the joint covariance, except in a minority of unique geometry conjunctions. For conjunctions with the right combination of orbital and drag characteristics, the cross-correlation effect can be substantial, though there are many conjunctions with marginal EDR for which this is not the case. For satellites with elevated EDR, the effect appears to be significant in terms of a factor of 1/2 or 2 change in about 1/3 of cases. Moreover, a positive outcome is that relatively few conjunctions exhibit factors much above 2, where the modified 2D-Pc is decidedly larger than that given by the current 2D-Pc. In this sense, 2D-Pc tends to be conservative, though overly so for many conjunctions with significant drag.

Finally, the ideal practical implementation of the modified formulation for Pc needs investigating. Though discussed in general herein, specific criteria for when the modification is warranted is of clear interest, in terms of EDR, prediction time, velocity geometry, etc. It is also of interest whether an EDR-based approach is feasible in practice. Otherwise, the full SP BFMC could be operationalized for this purpose, but might prove unwieldy across the hundreds of routine conjunctions worked daily. A longer term solution is to consider CDM additions for the required drag sensitivity vectors, along with accompanying DCP information, or even the deflated joint covariance itself. Also longer term, the overall phenomenon should continue to be examined and refined, particularly leading up to the next solar maximum in coming years, when average EDR levels will be much higher.

ACROYNMS

ASW = Astrodynamics Support Workstation
BFMC = Brute Force Monte Carlo
CARA = Conjunction Assessment and Risk Analysis
CDM = Conjunction Data Message
DCA = Dynamic Calibration Atmosphere
DCP = Dynamic Consider Parameter
EDR = Energy Dissipation Rate
GCP = Global Consider Parameter
GP = General Perturbations
ISS = International Space Station
OD = Orbit Determination
SP = Special Perturbations
TCA = Time of Closest Approach
VCM = Vector Covariance Message

REFERENCES

[1] J.L. Foster and H.S. Estes, "A Parametric Analysis of Orbital Debris Collision Probability and Maneuver Rate for Space Vehicles," NASA/JSC-25898, Aug. 1992.

[2] V.T. Coppola, J. Woodburn, and R. Hujsak, "Effects of Cross Correlated Covariance on Spacecraft Collision Probability," *AAS/AIAA Spaceflight Mechanics Meeting*, Wailea Maui, HI, Paper 04-181, Feb. 2004.

[3] S.J. Casali and W.N. Barker, "Dynamic Calibration Atmosphere (DCA) for the High Accuracy Satellite Drag (HASDM)," *AAS Astrodynamics Specialist Conference*, Monterey, CA, Paper 2002-4888, Aug. 2002.

[4] D.T. Hall, S.J. Casali, L.C. Johnson, B.B. Skrehart, and L.G. Baars, "High Fidelity Collision Probabilities Estimated Using Brute Force Monte Carlo Simulations," *AAS Astrodynamics Specialist Conference*, Snowbird, UT, Paper 18-244, Aug. 2018.

[5] R. Bate, D. Mueller, and J. White, *Fundamentals of Astrodynamics*, Dover Publications Inc., New York, 1971.